*Macromolecules* **1992,** *25,* 5597–5600

# Microstructural Analysis of Ethylene–Vinyl Acetate Copolymer by 2D NMR Spectroscopy

**Kebede Beshah**

*Rohm and Haas Research Laboratories, 727 Norristown Road,*
*Spring House, Pennsylvania 19477*

*Received April 30, 1992; Revised Manuscript Received June 30, 1992*

ABSTRACT: The comonomer sequences of ethylene–vinyl acetate copolymer have been analyzed by a novel approach that utilizes two-dimensional heteronuclear single quantum coherence and total correlation spectroscopy (2D HSQC-TOCSY). The combined carbon–proton and proton–proton correlations in a single 2D experiment enables a *direct* correlation among neighboring species. Hence, it is independent of the estimations of chemical shifts and peak intensities that are requisites of conventional procedures. Moreover, the proton–detected heteronuclear correlation experiment takes advantage of the high resolution of $^{13}C$ as well as the high sensitivity of $^1H$ NMR spectroscopy. As a result, it was possible to obtain improved assignments and much more detailed microstructural information.

## Introduction

High-resolution $^1H$ and $^{13}C$ NMR spectroscopy, and more recently multidimensional homonuclear and heteronuclear correlations spectroscopy, have revealed detailed structural features of complex polymers.[1–8] Microstructural features such as stereochemical configurations and comonomer sequences which give detailed insight into the mechanism of copolymerization including reactivity ratios are provided almost exclusively by NMR techniques.

Currently established procedures to determine microstructures of copolymers require most or all of the following steps:[8,9] (i) synthesis of model oligomers or copolymers with a series of relative concentrations, (ii) estimation of the chemical shifts of particular species in comonomer sequences from empirical additive rules,[10,11] (iii) estimation of relative intensities assuming Bernoullian or Markovian propagation statistics. This conventional technique has been successfully applied to provide microstructures of some copolymer systems.[9,12] However, there are some drawbacks to the universal implementation of the technique such as (i) the synthesis and assignment procedures are tedious and become extremely complicated with complex polymerizations involving multimonomers, (ii) chemical shifts are mostly dependent on the nature of solvent, temperature, pH, and impurity materials such as paramagnetic species and, as a result, it becomes difficult to use literature values for the empirical rules, (iii) stereochemical configuration and comonomer sequencing produce similar intensities for many sequence probabilities, hence assignment of comonomer sequences based on the theoretical fit of peak intensities may have some ambiguities.

Ideally, such sequence determination is best done by establishing a direct connectivity between neighboring species. $^{13}C$ 2D INADEQUATE NMR,[13] which correlates directly bonded $^{13}C$ pairs, has been effectively applied to determine comonomer sequences of stereoregular copolymers.[6,14,15] For a polymer with natural-abundance $^{13}C$, only one in $10^4$ carbon–carbon pairs are detected by this technique. Hence, the technique has poor sensitivity and is applicable for some special cases with stereoregular structures.

In this work, it is shown how a 2D technique that couples single-bond carbon–proton correlation together with proton–proton correlation spectroscopy can provide an absolute determination of microstructural features of copolymers. Since both heteronuclear (C–H) and homonuclear (H–H) correlations are established in a single 2D experiment with a proton detection scheme, the resulting data have the high resolution of $^{13}C$ spectrum and the high sensitivity of proton nuclei. The peak assignments are made independent of empirical chemical shift rules and propagation statistics which allow a choice of experimental conditions (solvent, temperature, pH, shift reagents, etc.) that best suit the particular polymer system being investigated. This direct technique is applied to ethylene–vinyl acetate (EVa) copolymer. A substantial amount of work has been done to characterize the microstructures of EVa copolymer.[8,16–19] The direct method of establishing neighbors employed in the current work has enabled umambiguous assignments of additional features of the microstructures of EVa.

## Experimental Section

Ethylene–vinyl acetate copolymer was purchased from Scientific Polymer Products Inc. as part of a polymer sample kit. The 60/40 EVa has a molecular weight ($M_w$) of 110 000. A 15–20% solution of the sample was prepared in 1,2,4-trichlorobenzene with a small amount of benzene-$d_6$ for the deuterium lock signal.

The NMR experiments were done on a Bruker AMX500 spectrometer with a reverse ($^1H$ detection) probe. The heteronuclear single quantum coherence (HSQC) experiment[20] with proton detection scheme has high sensitivity and allows a second polarization transfer step (TOCSY)[21,22] among the proton spins, making sequential assignments possible. Thus, the spectra obtained by the 2D HSQC-TOCSY experiment show signals that arise from single-bond heteronuclear (C–H) as well as three-bond homonuclear (H–H) correlations. For example, in a spectrum of a vinyl polymer with a $-CH_2-CH-$ backbone repeat unit, at least two sets of cross peaks are expected along each of the methylene and methine carbon resonances. In the case of the methylene carbon, one set of cross peaks correlate it to the directly bonded methylene protons and the other to the neighboring methine protons, establishing the sequence. In the case of a comonomer sequence, an additional set of cross peaks is observed to the resonances of the neighboring comonomer. The sequential assignment is repeated along the polymer chain for the direct determination of microstructures.

It is emphasized that the TOCSY transfer step is done with a spin lock field; hence there is minimal magnetization decay from the characteristic short $T_2$ of macromolecules. The magnetization transfer time (mix time) for the proton–proton correlations can be adjusted for establishing nearest as well as next nearest neighbors. In this work a mix time of 19.8 ms was utilized in order to observe only three-bond proton–proton correlations.

The 2D NMR data acquisition times can be reduced significantly (for example, to a couple of hours for the single-bond

0024-9297/92/2225-5597$03.00/0 © 1992 American Chemical Society

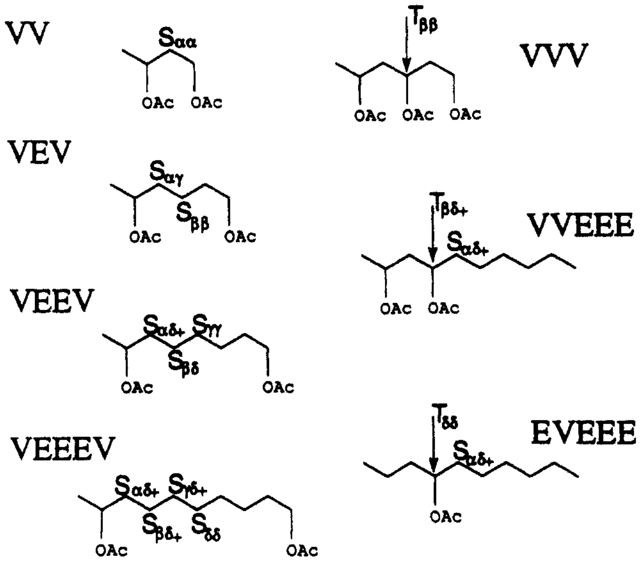

**Figure 1.** Nomenclature of ethylene–vinyl acetate copolymers. Magnetically inequivalent primary (P), secondary (S), and tertiary (T) carbons are identified by Greek subscripts indicating the nearest tertiary carbon positions.

heterocorrelation experiment), if fairly concentrated (viscous) solutions are prepared in appropriate solvent(s). Such high concentrations introduce minimal broadening of the line width since the local segmental motion which is responsible for the broading of the line width is not significantly affected by concentration.

## Results and Discussion

**Nomenclature.** The sequential assignment is facilitated by the use of consistent nomenclature[8,23] developed for the variety of magnetically nonequivalent secondary and tertiary carbons that result from copolymerization. In this nomenclature, Greek subscripts indicate the positions of the nearest tertiary carbons from the secondary (S) or tertiary (T) positions of the backbone carbons. Figure 1 illustrates the nomenclature for most of the nonequivalent S and T species in the building blocks of the ethylene–vinyl acetate copolymer.

**Spectral Assignment.** The assignment of peaks will be made in several self-consistent stages that exploit the neighboring arrangements of the carbon moieties in the microstructures. At each stage, the assignments will be based on the direct experimental data obtained in this work without any reference to previous assignments made by other workers.

**Stage 1.** In the first stage, a one-dimensional $^{13}$C DEPT[24] experiment (Figure 2) was used to assign secondary (S) carbon signals from 21 to 40 ppm, tertiary (T) carbon signals from 65 to 75 ppm, and the primary (P) or methyl carbon signal at 21 ppm. For a more complicated spectrum with severe spectral overlap, a C–H-coupled ($^1J_{CH}$) heteronuclear 2D correlation experiment can be used to distinguish P, S, and T carbons.

**Stage 2.** At this stage, a single-bond carbon–proton correlation is made, as shown in Figure 3. The secondary carbons are correlated to the proton resonances at 1–2 ppm, while the tertiary carbons are correlated to protons at about 5 ppm. Note that it is not possible to distinguish between methylene resonances without additional experiments and estimations, as outlined in the Introduction. As shown in the next stage, the spectrum in Figure 3 is used to distinguish single-bond carbon–proton correlations from those of neighboring nuclei.

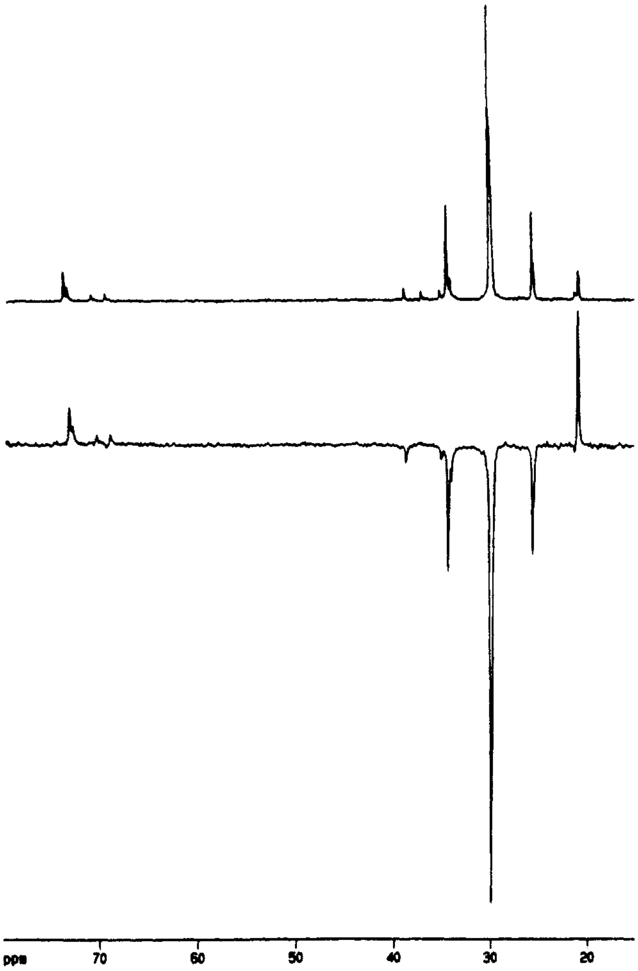

**Figure 2.** $^{13}$C spectra of ethylene–vinyl acetate copolymer. The bottom spectrum ($^{13}$C DEPT) differentiates the tertiary carbons (above 60 ppm) from the secondary carbons (21–45 ppm, inverted) and the methyl carbon at 21 ppm.

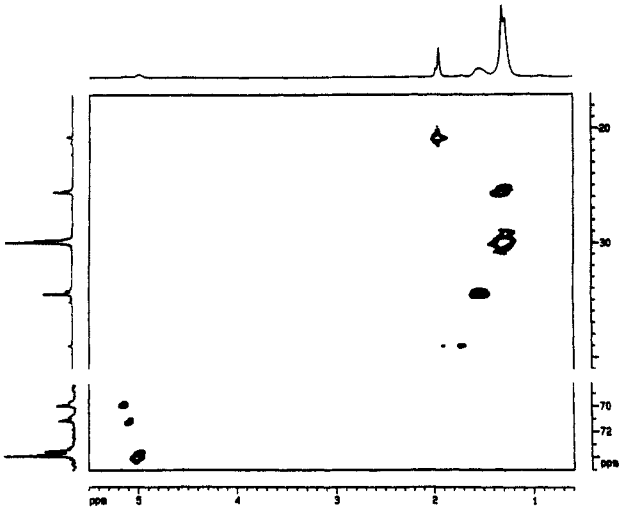

**Figure 3.** Single-bond C–H correlation 2D HSQC spectrum of ethylene–vinyl acetate copolymer. The low-field tertiary carbon region has been expanded for clarity.

**Stage 3.** A second 2D spectrum (Figure 4) is obtained by the HSQC-TOCSY experiment. The additional peaks observed in this spectrum (compared to Figure 3) are due to the three-bond proton–proton correlation peaks attained in the TOCSY step of the experiment. For example, the tertiary $^{13}$C peak at 69.6 ppm has two cross peaks at 5.1 and 1.7 ppm, correlating it to directly attached protons (stage 2) and neighboring methylene protons, respectively. In the following paragraphs, a step by step assignment of the comonomer sequences is made from the carbon–proton and proton–proton correlation signals.

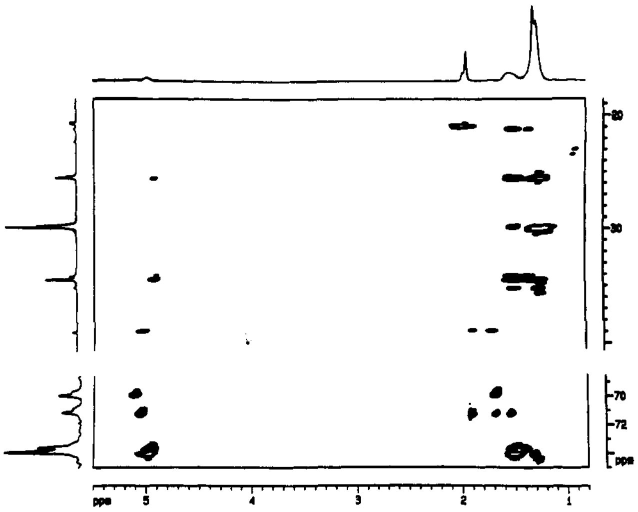

**Figure 4.** 2D HSQC-TOCSY spectrum of ethylene vinyl acetate. In addition to the single-bond C–H correlations (Figure 3), next neighbor correlations are established by the TOCSY step of the experiment. Higher digital resolution was used in the carbon dimension in order to observe detailed features of the correlation step. Similar to Figure 3, the tertiary carbon region has been expanded for clarity.

(i) The secondary carbon peaks at 30 ppm do not show any correlation to the methine protons at about 5 ppm. Thus this set of peaks has to be farther from tertiary carbons; as a result, they are assigned to $S_{\delta\delta}$, $S_{\gamma\gamma}$, and $S_{\gamma\delta}$. There is additional correlation between the upfield shoulder peak at 29.9 ppm and the methylene protons at 1.5 ppm. From Figure 3 it has already been observed that the methylene protons at 1.5 ppm are directly bonded to the secondary carbons at 34.5 ppm. Hence, the upfield shoulder signal at 29.7 ppm has to be from a methylene carbon near neighbor to the methylene carbon at 34.5 ppm. This information and the subsequent assignments will be used to differentiate between $S_{\delta\delta}$ and $S_{\gamma\delta}$. It should be noted that $S_{\beta\beta}$ is not also expected to show any correlations with the methines. But its assignment to the set of peaks at 30 ppm is excluded by subsequent analysis (see step vii below).

(ii) The secondary carbon at 39 ppm that does not show any correlation to the rest of the secondary carbons is assigned to $S_{\alpha\alpha}$. From the structure in Figure 1, we realize $S_{\alpha\alpha}$ is the only secondary carbon that is sandwiched between two tertiary carbons. Hence, $S_{\alpha\alpha}$ is not expected to show any significant correlation to protons of other secondary carbons under the current experimental conditions.

(iii) One of the methine carbons at 69.6 ppm shows a strong correlation to only $S_{\alpha\alpha}$ protons at 1.66 ppm. According to the structure, $S_{\alpha\alpha}$ is the only secondary carbon that is nearest neighbor to $T_{\beta\beta}$. Thus the tertiary carbon at 69.9 ppm with unique correlation to $S_{\alpha\alpha}$ is assigned to $T_{\beta\beta}$. Similarly, the only other tertiary carbon (71.1 ppm) that also exhibited correlation to $S_{\alpha\alpha}$ is assigned to $T_{\beta\delta}$.

(iv) The $T_{\beta\delta}$ peak at 71.1 ppm shows correlations to two neighboring protons at 1.5 and 1.66 ppm in addition to the correlation to the directly bonded methine proton at 5.05 ppm. The structure (Figure 1) shows that $T_{\beta\delta}$ can have only $S_{\alpha\alpha}$ and $S_{\alpha\delta}$ and/or $S_{\alpha\gamma}$ as its neighbors. In step iii we have already established the correlation to the neighboring $S_{\alpha\alpha}$ at 1.66 ppm. The remaining proton neighbor at 1.55 ppm with the corresponding carbon signal at 34.5 ppm is assigned to $S_{\alpha\delta}$ and/or $S_{\alpha\gamma}$.

(v) The remaining tertiary carbon peaks at 73–74 ppm are assigned to $T_{\delta\delta}$ on the basis of their correlations to $S_{\alpha\delta}$ and/or $S_{\alpha\gamma}$ (34.5 ppm). Note that $T_{\delta\delta}$ and $T_{\beta\delta}$ (step iv) are the nearest neighbors of $S_{\alpha\delta}$ and/or $S_{\alpha\gamma}$.

(vi) Finally, $S_{\beta\delta}$ at about 26 ppm is identified from the correlations to its neighbor protons of $S_{\alpha\delta}$ and $T_{\delta\delta}$.

(vii) $S_{\alpha\gamma}$ and $S_{\beta\beta}$ are readily identified since they are the only unique secondary carbon neighbors sandwiched between tertiary carbons in the VEV segment of the sequence. Figure 5 illustrates the correlation of $S_{\alpha\gamma}$ at 1.55, 34.23 ppm to $S_{\beta\beta}$ at 1.45, 21.3 ppm. In addition, the figure shows the correlation of $S_{\alpha\delta}$ (1.55, 34.5) and an unassigned resonance at 35.2 ppm (see next stage) to $S_{\beta\delta}$ protons at 1.35 ppm.

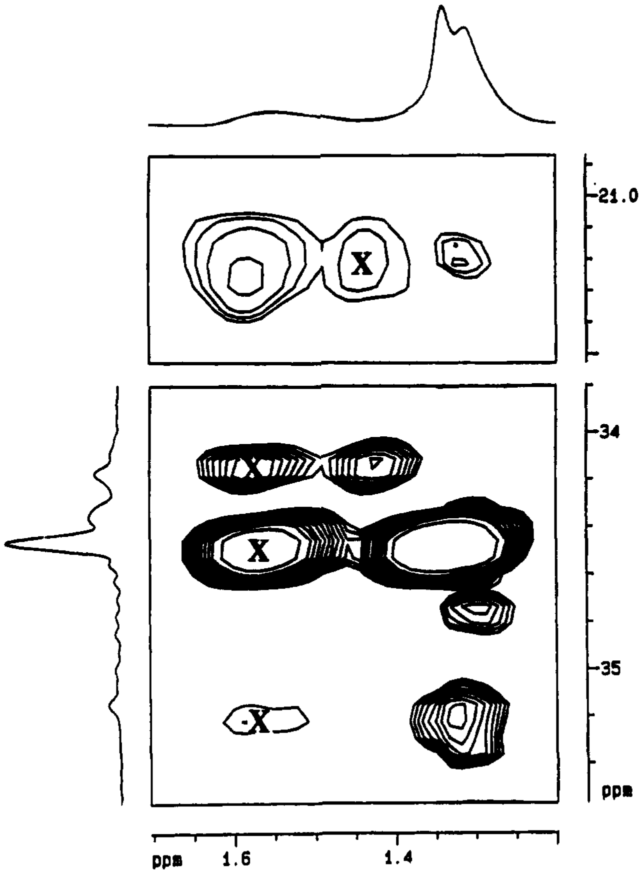

**Figure 5.** Expanded region of Figure 4 showing the correlations of $S_{\alpha\delta}$, $S_{\alpha\gamma}$, and $S_{\beta\beta}$. The correlation between $S_{\beta\beta}$ (1.45, 21.5) and $S_{\alpha\gamma}$ (1.55, 34.2) is clearly observed in this plot. The correlations of $S_{\alpha\delta}$ (1.55, 34.6) and the unique resonance (see text) at 1.55, 35.3 ppm to $S_{\beta\delta}$ at 1.35 ppm is illustrated. The single-bond correlation peaks are indicated by x.

**Stage 4.** Once the major groups of peaks are assigned to the major microstructural features, more detailed information is obtained from an expanded plot of the peaks arising from the correlation of secondary carbons and the methine protons, as shown in Figure 6.

The major peak of $S_{\beta\delta}$ shows a strong correlation to $T_{\delta\delta}$ protons (Figure 6A), indicating the predominant sequence segment of EVEE. The smaller $S_{\beta\delta}$ peak at 25.4 ppm is correlated to $T_{\beta\delta}$ (about 5.1 ppm). Clearly, the two carbon moieties are part of the VVEE segment.

Figure 6B illustrates the region of the spectrum correlating $S_{\alpha\beta}$, $S_{\gamma\gamma}$, and $S_{\alpha\gamma}$ to the protons of tertiary carbons. Similar to Figure 6A, the most intense cross peak is correlated to $T_{\delta\delta}$, indicating EVEE as the most abundant sequence segment. The small cross peak at 5.1 ppm correlates $S_{\alpha\delta}$ to $T_{\beta\delta}$ in a VVEE segment of the sequence. The most upfield cross peak at 34.2 ppm correlates $S_{\alpha\gamma}$ to $T_{\delta\delta}$ in an EVEV segment.

The most downfield shifted cross peak at 5.15, 35.3 ppm in Figure 6B correlates a secondary carbon, possibly $S_{\alpha\delta}$,

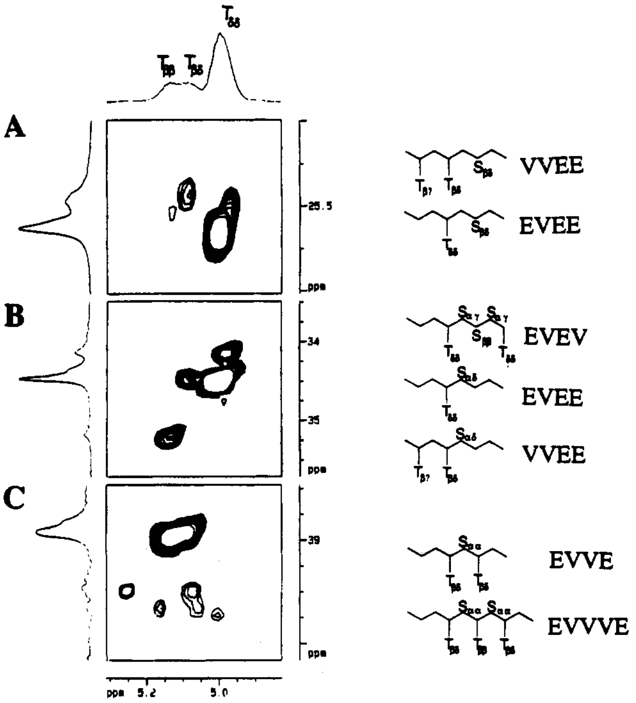

**Figure 6.** Expanded regions of Figure 4 illustrating detailed correlations of $S_{\beta\delta}$ (A), $S_{\alpha\delta}$, $S_{\alpha\gamma}$ (B), and $S_{\alpha\alpha}$ (C). See text for assignment.

to methine protons similar to $T_{\beta\beta}$, as determined by the proton chemical shift at 5.15 ppm. Such correlation does not fit well with the regular comonomer sequences. More work is needed to get a direct assignment of this signal arising from a seemingly irregular structure such as monomer inversion of vinyl acetate in a VV segment.

Finally, Figure 6C illustrates the correlation of $S_{\alpha\alpha}$ to methine protons. The crosspeak at 39 ppm with correlations to $T_{\beta\delta}$ and $T_{\beta\beta}$ peaks is consistent with the EVVVE segment of the copolymer sequence. The skewed crosspeak indicates the correlation of the upfield shoulder peak of $S_{\alpha\alpha}$ to $T_{\beta\delta}$, as expected for the EVVE segment. Much weaker crosspeaks are also observed at about 39.5 ppm. Similar to the weak signal in Figure 6B, the characterization of these weak peaks suffers from a dynamic range problem and work is underway to determine the microstructures responsible for these signals by direct experimental measurement similar to the one outlined in this work.

A summary of the $^{13}$C chemical shift assignments together with the structural block segment to which the carbon moiety belongs is summarized in Table I.

## Conclusion

The comonomer sequences of ethylene–vinyl acetate copolymer have been determined from sequential assignments based on the correlation of both heteronuclear (C–H) and homonuclear (H–H) connectivities of neighboring species in a single 2D NMR experiment. The high resolution and sensitivity of the 2D HSQC-TOCSY experiment provided a detailed microstructural analysis. In addition, the direct assignments of comonomer sequences based on correlations of neighboring species makes this approach reliable since it is independent of chemical shift and peak intensity estimates by empirical rules.

**Table I**
**$^{13}$C Chemical Shift Assignment of Ethylene–Vinyl Acetate Copolymers**

| carbon | moiety | structure segment | $^{13}$C chemical shift (ppm) |
|---|---|---|---|
| $CH_3O$ | P | V | 20.9 |
| $CH_2$ | $S_{\beta\beta}$ | VEV | 21.3 |
| $CH_2$ | $S_{\beta\delta}$ | EVEE | 25.4 |
| $CH_2$ | $S_{\beta\delta}$ | VVEE | 25.7 |
| $CH_2$ | $S_{\gamma\delta}$ | VEEE | 29.9 |
| $CH_2$ | $S_{\delta\delta}$, $S_{\gamma\gamma}$ | EEEE, EE | 30.1 |
| $CH_2$ | $S_{\alpha\gamma}$ | EVEV | 34.2 |
| $CH_2$ | $S_{\alpha\delta}$ | VVEE | 34.5 |
| $CH_2$ | $S_{\alpha\delta}$ | EVEE | 34.6 |
| $CH_2$ | $S_{\alpha\delta}$[a] | | 35.3 |
| $CH_2$ | $S_{\alpha\alpha}$ | EVVE | 39 |
| $CH_2$ | $S_{\alpha\alpha}$ | VVVE | 39.5 |
| CH | $T_{\beta\beta}$ | VVV | 69.3–69.7 |
| CH | $T_{\beta\delta}$ | VV and VVV | 70.6–71.1 |
| CH | $T_{\delta\delta}$ | EVEE | 73.4–74 |

[a] Irregular sequence (see text).

Clearly, these features are ideal for the characterization of complex polymers consisting of several monomers.

The direct detection of neighboring species permits the characterization of other microstructural features such as stereochemical configuration and conformation, regioirregularity, graft and branch sites, endgroup identification, and small molecule byproducts (mono and diadducts) of the polymerization reaction.

**Acknowledgment.** I thank Dr. P. O. Danis for donating the EVa sample and Dr. S. K. Wolk for stimulating discussions.

## References and Notes

(1) Bovey, F. A. *Nuclear Magnetic Resonance Spectroscopy*, 2nd ed.; Academic Press: New York, 1988.
(2) Bruch, M. D.; Bovey, F. A. *Macromolecules* **1984**, *17*, 978.
(3) Bruch, M. D.; Bovey, F. A.; Cais, R. E. *Macromolecules* **1984**, *17*, 2547.
(4) Mirau, P. A.; Bovey, F. A. *Macromolecules* **1986**, *19*, 210.
(5) Crowder, M. W.; Szeverenyi, N. M.; Levy, G., C. *Macromolecules* **1986**, *19*, 1333.
(6) Aoki, A.; Hayashi, T.; Asakura, T. *Macromolecules* **1992**, *25*, 155.
(7) Hikichi, K.; Yasuda, M. *Polym. J.* **1987**, *19*, 1003.
(8) Cheng, H. N.; Lee, G. H. *Macromolecules* **1988**, *21*, 3164.
(9) Randall, J. C. *Polymer Sequence Determination, Carbon-13 NMR Method*; Academic Press: New York, 1977.
(10) Grant, D. M.; Paul, E. G. *J. Am. Chem. Soc.* **1964**, *86*, 2984.
(11) Tonelli, A. E. *Macromolecules* **1978**, *11*, 565.
(12) Cheng, H. N. *J. Polym. Sci. Polym. Phys. Ed.* **1983**, *21*, 573.
(13) Bax, A.; Freeman, R.; Kempsell, S. P. *J. Am. Chem. Soc.* **1980**, *102*, 4849.
(14) Hikichi, K.; Hirai, T.; Ikura, M.; Higuchi, K.; Ohuchi, M. *Polym. J.* **1987**, *19*, 1317.
(15) Hayashi, T.; Inouye, Y.; Chujo, R.; Asakura, T. *Polym. J.* **1988**, *20*, 895.
(16) Schaefer, J. *J. Phys. Chem.* **1966**, *70*, 1975.
(17) Wu, T. K.; Ovenall, D. W.; Reddy, G. S. *J. Polym. Sci., Polym. Phys. Ed.* **1974**, *12*, 901.
(18) Delfini, M.; Segre, A. L.; Conti, F. *Macromolecules* **1973**, *6*, 456.
(19) Cheng, H. N.; Lee, G. H. *Polym. Bull.* **1988**, *19*, 89.
(20) Bodenhausen, G.; Ruben, D. J. *Chem. Phys. Lett.* **1980**, *69*, 185.
(21) Braunschweiler, L.; Ernst, R. R. *J. Magn. Reson.* **1983**, *53*, 521.
(22) Davis, D. G.; Bax, A. *J. Am. Chem. Soc.* **1985**, *107*, 2820.
(23) Carman, C. J.; Harrington, R. A.; Wilkes, C. E. *Macromolecules* **1977**, *10*, 536.
(24) Doddrell, D. M.; Pegg, D. T.; Bendall, M. R. *J. Magn. Reson.* **1982**, *48*, 323.

**Registry No.** (Ethylene)(vinyl acetate) (copolymer), 24937-78-8.